Film Thickness in Elastohydrodynamically Lubricated Slender Elliptic Contacts: Part I - Numerical Studies of Central Film Thickness

Marius Wolf, Sergey Solovyev, Arshia Fatemi
Corporate Research Robert Bosch GmbH

Abstract

In this paper, analytical equations for the central film thickness in slender elliptic contacts are investigated. A comparison of state-of-the-art formulas with simulation results of a multilevel EHL solver is conducted and shows considerable deviation. Therefore, a new film thickness formula for slender elliptic contacts with variable ellipticity is derived. It incorporates asymptotic solutions, which results in validity over a large parameter domain. It captures the behaviour of increasing film thickness with increasing load for specific very slender contacts. The new formula proves to be significantly more accurate than current equations. Experimental studies and discussions on minimum film thickness will be presented in a subsequent publication.

Introduction

Fluid film thickness equations are the main bridge between scientific studies on elastohydrodynamic and its engineering applications in gears and rolling element bearings. The first mathematical film thickness formulation for highly concentrated contacts is proposed in the seminal work of Dowson and Higginson for minimum film thickness in 1961 [1] and Dowson and Toyoda for central film thickness [2] both for line contacts. They formulated the dimensionless film thickness H as a function of three dimensionless parameters of material (G), speed (U) and load (W), which were easy to use, physically making sense and are nowadays immensely established in application. Two decades later, Hamrock and Dowson published a series of papers [3, 4, 5, 6], regarding elliptic contacts, systematically investigating effects of ellipticity as well as above mentioned parameters. More recently, Lubrecht et al. [7] revisited the equations developed above with higher computational power and finer numerical precision. The investigators have been astonished by confirmation the precision of the equations for line contact developed 50 years prior to their investigation and commented about minor academic issues.

However, before these investigations Ranger et al. [8] at imperial college were the first group who developed a numerical equation for line and point contacts. Yet, their work has not been appreciated because it predicts a counter-intuitive behaviour of increasing film thickness with increasing load within the parameter range of their studies. Recently, this behaviour has been verified and explained [9].
In 1992 Moes [10] adopted the optimum similarity analysis to the domain of lubricated contacts and reduced the number of non-dimensional parameters to two (L and M). By incorporation of asymptotic solutions for different lubrication regimes, the outreach of line contact film thickness equation is extended to isoviscous-elastic, piezoviscous-rigid and isoviscous-rigid regimes. Adopting the methodology of Moes, Nijenbanning et al. [11] solve EHL equations numerically for wide elliptic contacts and for a large number of combinations of M and L, which have been addressed extensively in this paper.
Due to its more widespread application in rolling element bearings, the above mentioned equations focus prevalently on wide elliptic contacts e.g., the entrainment velocity is in the direction of the minor contact ellipse axis. Slender elliptic contacts have been less subject to systematic studies and film thickness equations are not optimised to cover this particular shape of contacts and its domain of parameters. The major significant work on film thickness of slender contacts is based on the extensive study of Chittenden et al. [12, 13] using the same numerical algorithm of Hamrock and Dowson. In addition, Moes [14] adapted the formula of Nijenbanning et al. [11] to general elliptic contacts, however, the deviation between these formulas is negligible. Within this paper, slender contacts are defined as elliptic contact with entrainment velocity directed along the major axis of the contact ellipse. These contacts occur, for example, at the roller-flange interface within cylindrical or tapered roller element bearings or within worm gears and are therefore a highly relevant field of research [15, 16, 17].
In this paper the problem of analytical film thickness expressions for slender elliptic contacts is revisited. The focus lies on the central film thickness, which is commonly used for analytical prediction of friction forces in lubricated contacts, since it represents the major part of the contact area and the high pressure region [18, 19, 20, 21]. The central film thickness is defined as the film thickness at the location of maximum fluid pressure [11, 14].

Simulation Model

The EHL simulations were performed with a multilevel EHL solver analogous to the work of Venner and Napel [22]. Detailed descriptions of the working principle of EHL solvers can be found in the literature [23, 24] and are therefore not given here.
The following assumptions are made:

- fluid incompressibility
- smooth surfaces / no solid contact
- steady state

- isothermal behaviour
- fully-flooded contact / no starvation
- Newtonian behaviour
- Barus pressure-viscosity law $\eta(p) = \eta_0 \exp(\alpha p)$

The assumptions towards the fluid properties are discussed in a subsequent section. The assumptions hold valid, if compressibility is considered via a correction factor (eq. 13). As shown by Moes [10], the problem can be reduced to the dimensionless parameters

$$H = \frac{h}{R_\mathrm{e}} \left(\frac{\eta_0 u_0}{E' R_\mathrm{e}} \right)^{-1/2} \tag{1}$$

$$M = \frac{F_\mathrm{N}}{E' {R_\mathrm{e}}^2} \left(\frac{\eta_0 u_0}{E' R_\mathrm{e}} \right)^{-3/4} \tag{2}$$

$$L = \alpha_\mathrm{p}^* E' \left(\frac{\eta_0 u_0}{E' R_\mathrm{e}} \right)^{1/4} . \tag{3}$$

As recommended by Vergne and Bair [25], the reciprocal asymptotic isoviscous pressure coefficient α_p^* as defined by Blok [26] is used for film thickness modelling. It is defined as

$$\alpha_\mathrm{p}^* = \left(\int_{0.1\,\mathrm{MPa}}^{\infty} \frac{\eta_0}{\eta(p)} \mathrm{d}p \right)^{-1} \tag{4}$$

with η_0 as the viscosity at ambient pressure. Fluid modelling using Barus pressure-viscosity law leads to $\alpha_\mathrm{p}^* = \alpha$.
These parameters and the ellipticity parameter, defined as the ratio of the reduced radii of curvature,

$$D = \frac{R_\mathrm{e}}{R_\mathrm{s}} \tag{5}$$

are used for contact characterization within this paper. R_e and R_s represent the effective radii in direction of entrainment velocity (R_e) and transverse to it (R_s). The effective radius in direction i can be calculated via

$$1/R_i = 1/R_{i,1} + 1/R_{i,2}. \tag{6}$$

A detailed definition of the variables can be found in the nomenclature.

State-of-the-art formulas

Following the pioneer work of Hamrock and Dowson [5] in 1977, many more analytical film thickness formulas for point and elliptic contacts were derived [10, 11, 12, 27, 28,

29, 30, 31]. A comprehensive overview is given by Marian et al. [32] and Van Leeuwen [33], which also provides a comparison to experimental data.
However, almost all approaches focus on point ($D = 1$) or wide elliptic contacts ($D < 1$). Only Chittenden et al. [12] consider slender contacts ($D > 1$). The authors also provides an analytical formula for arbitrary entrainment angles [28]. It is more commonly used in literature and is therefore benchmarked against EHL simulations. In order to investigate, whether or not analytical formulas for wide contacts can be extrapolated to slender contacts, the film thickness formula of Nijenbanning et al. [11] is reviewed as well. This formula is chosen, since it integrates the asymptotic behaviour and is therefore expected to be valid for a greater range of parameters compared to other approaches.

Chittenden et al. [28]

Chittenden et al. use the dimensionless parameters

$$U = \frac{\eta_0 u_0}{2E' R_\mathrm{e}} \tag{7}$$

$$G = \alpha_\mathrm{p}^* E' = L(2U)^{-1/4} \tag{8}$$

$$W = \frac{F_\mathrm{N}}{E' {R_\mathrm{e}}^2} = M(2U)^{3/4} \tag{9}$$

and

$$\tilde{H}_\mathrm{C} = \frac{h}{R_\mathrm{e}} = H(2U)^{1/2}. \tag{10}$$

The film thickness formula for arbitrary entrainment angels reads

$$\tilde{H}_\mathrm{C} = 4.31 G^{0.49} U^{0.68} W^{-0.073} \left[1 - \exp\left(-1.23 \left(\frac{R_\mathrm{s}}{R_\mathrm{e}}\right)^{\frac{2}{3}}\right)\right] \tag{11}$$

with

$$\frac{R_\mathrm{s}}{R_\mathrm{e}} = \frac{\frac{R_\mathrm{y}}{R_\mathrm{x}} \sin^2\theta + \cos^2\theta}{\frac{R_\mathrm{y}}{R_\mathrm{x}} \cos^2\theta + \sin^2\theta} \tag{12}$$

and θ as the angle between the entrainment velocity and the major axis (x-axis) of the contact ellipse. It must be noted that Chittenden et al. [28] are using training data obtained by simulations with compressible fluids and Roelands [34] behaviour for the pressure-viscosity relationship. While the kind of used pressure-viscosity law has no significant effect on film thickness, (in)compressibility must be considered, when comparing different approaches. Therefore, correction via

$$H_\mathrm{com} = \frac{H_\mathrm{inc}}{\bar{\rho}(p_\mathrm{H})} \tag{13}$$

with the pressure-density law of Dowson and Higginson [35, 36]

$$\bar{\rho}(p) = \frac{\rho(p)}{\rho_0} = \frac{b + cp}{b + p} \tag{14}$$

is used [31]. p_H refers to the maximum Hertzian pressure. In accordance to the work of Chittenden et al. [28], the parameters are set to $b = 5.9 \times 10^8\,\mathrm{Pa}$ and $c = 1.34$.
For comparison, H as defined by Moes [10] from eq. 1 is used. Therefore, $\tilde{H}_\mathrm{C}$ from eq. 11 is multiplied by $(2U)^{-1/2}$ beforehand.

Nijenbanning et al. [11]

The film thickness formula of Nijenbanning et al. [11] is based on the same assumptions as the EHL simulations of this paper. It was derived for wide elliptic contacts ($D < 1$) and reads:

$$H_\mathrm{N} = \left\{ \left[H_\mathrm{N,IR}^{1.5} + \left(H_\mathrm{N,IE}^{-4} + H_\mathrm{N,00}^{-4} \right)^{-3/8} \right]^{2s/3} + \left[H_\mathrm{N,PE}^{-8} + H_\mathrm{N,PR}^{-8} \right]^{-s/8} \right\}^{1/s} \tag{15}$$

with

$$H_\mathrm{N,IR} = 145 \left(1 + 0.796 D^{14/15} \right)^{-15/7} D^{-1} M^{-2} \tag{16}$$

$$H_\mathrm{N,IE} = 3.18 \left(1 + 0.006 \ln(D) + 0.63 D^{4/7} \right)^{-14/25} \cdot D^{-1/15} M^{-2/15} \tag{17}$$

$$H_\mathrm{N,PR} = 1.29 \left(1 + 0.691 D \right)^{-2/3} L^{2/3} \tag{18}$$

$$H_\mathrm{N,PE} = 1.48 \left(1 + 0.006 \ln(D) + 0.63 D^{4/7} \right)^{-7/20} \cdot D^{-1/24} M^{-1/12} L^{3/4} \tag{19}$$

$$H_\mathrm{N,00} = 1.8 D^{-1} \tag{20}$$

$$s = 1.5 \left[1 + \exp\left(-1.2 \frac{H_\mathrm{N,IE}}{H_\mathrm{N,IR}} \right) \right]. \tag{21}$$

Benchmarking

First, the presented film thickness formulas are tested for wide elliptic contacts in order to evaluate both the quality of the film thickness formulas and the quality of the used EHL solver. The results are shown for different values of M and L and an ellipticity ratio of $D = 0.25$ in fig. 1.
It can be seen that the formula of Chittenden et al. [28] (eq. 11) only shows partial consistency for medium values of M and medium to large values of L. It fails to predict

the film thickness for small values of both M and L. This becomes especially evident for the case of $L = 0$: Eq. 11 predicts $H = 0$, which is clearly not the case. This comparison does not claim to be an exhaustive evaluation of the film thickness formula of Chittenden et al. [28], which was not derived for the entire investigated L and M parameter range. Instead, it investigates its general capability to predict the film thickness in elliptic contacts. For a complete evaluation, results of EHL simulations with compressible fluids instead of correction via eq. 13 are required.
In contrast, excellent agreement with a slight tendency towards overestimation is given between the EHL simulations and the formula of Nijenbanning et al. [11]. Especially the asymptotic behaviour for $L = 0$ and $M \to 0$ is captured in a superior way compared to Chittenden et al. [28]. The precise conformity between Nijenbanning et al. [11] and the employed EHL solver (avg. relative error of 3.43%) is a strong indication for correct functioning of the EHL solver.
Wheeler et al. [13] observe a significant systematic overestimation of the film thickness by the formula of Nijenbanning et al. [11]. This contradicts the findings of this paper. However, the overestimation occurred, when comparing the Nijenbanning formula with compressible EHL simulations. Since the model of Nijenbanning et al. [11] assumes incompressibility and no correction factor was applied, the overestimation is explainable and expected.
Following the benchmarking of wide elliptic contacts, the film thickness formulas are also evaluated for slender elliptic contacts. The results for a wide range of M and L values are shown in fig. 2 ($D = 2$) and fig. 3 ($D = 5$). As for wide elliptic contacts, the formula of Chittenden et al. [28] only correctly captures the behaviour for medium values of both M and L. For simulations with $L \neq 0$, the average relative error is 15.3 % ($D = 2$) and 17.8 % ($D = 5$), respectively and 100 % for $L = 0$. The quality of the prediction of Nijenbanning et al. [11] declines with increasing ellipticity as a result of stronger extrapolation from its training range. The average relative error is only 5.44 % for $D = 2$, whereas it increases to 18.7 % for $D = 5$.
This comparison demonstrates the necessity of a new film thickness formula for slender elliptic contacts with validity over a broad parameter domain.

New Film Thickness Formula for Slender Contacts

The focus of this paper is to provide an easy-to-implement formula by using standard mathematical functions.
Johnson [37] distinguishes four different lubrication regimes:

1. Isoviscous-Rigid (small L and small M)
2. Isoviscous-Elastic (small L and large M)
3. Piezoviscous-Rigid (large L and small M)
4. Piezoviscous-Elastic (large L and large M)

Unlike for line contacts, the boundaries of the regime cannot be specified explicitly, since they depend on the ellipticity ratio D of the contact.
Solutions for the asymptotic behaviour of the film thickness in a point contact exist for each regime and are incorporated in the film thickness formula. The prefactors C_i of the asymptotic solutions are functions of the ellipticity ratio D and are derived by curve fitting a large number of simulations within each regime, resulting in an overall number of 2282 successfully converged simulations. The base form of each prefactor function is chosen individually to best match the ellipticity dependence. The coefficient were determined using a least squares regression approach.
The dimensionless values L, M and the ellipticity ratio D were varied within $L \in [0, 100]$, $M \in [0.5, 20000]$ and $D \in [1, 10]$. In order to avoid numerical influences on the quality of the simulation results, first the mesh density is increased until no significant change in the central film thickness can be observed any more. Afterwards, the simulation area is increased until again no change in the central film thickness occurs. It should be noted that for simulations with small M values, the required simulation area is many times larger than the Hertzian contact area, whereas for high M values a fine mesh is required.
The final form of the film thickness equation is analogous to Nijenbanning et al. [11]. It is a weighting of the contributions of different lubrication regimes and reads:

$$H = \left\{ \left[H_{\mathrm{IR}}^{1.73} + \left(H_{\mathrm{IE}}^{-1.33} + H_{00}^{-1.33} \right)^{-\frac{1.73}{1.33}} \right]^{\frac{t}{1.73}} + \left[H_{\mathrm{PE}}^{-13.8} + \left(H_{\mathrm{PR}}^{-24.1} + H_{\mathrm{M}}^{-24.1} \right)^{\frac{13.8}{24.1}} \right]^{-\frac{t}{13.8}} \right\}^{1/t} \tag{22}$$

with

$$H_{00} = 4.13 \cdot D^{-1} \tag{23}$$

$$t = \left[\left(1.43^{0.803} + \left(\frac{4.65}{M} \right)^{0.803} \right)^{-\frac{5}{0.803}} + 4^{-5} \right]^{-1/5} \tag{24}$$

as the transition parameters between the isoviscous-rigid and isoviscous-elastic (H_{00}) and between the isoviscous and piezoviscous regimes (t). The coefficients for weighting are based on simulations in between the lubrication regimes.
The partial solutions $H_{\mathrm{IR}}, H_{\mathrm{IE}}, H_{\mathrm{PR}}, H_{\mathrm{M}}$ and H_{PE} are defined in the following sections.

Isoviscous-Rigid

The load-free zone of roller element bearings is an example for the occurrence of isoviscous-rigid contacts. From a similarity analysis follows [11]

$$H_{\mathrm{IR}} \propto M^{-2}. \tag{25}$$

Curve fitting the prefactor C_{IR} leads to

$$H_{\mathrm{IR}} = C_{\mathrm{IR}}(D) \cdot M^{-2} \tag{26}$$

with

$$C_{\mathrm{IR}}(D) = 236\left(1 + 0.65D^{0.704}\right)^{-3.37} D^{-1}. \tag{27}$$

Isoviscous-Elastic

Contacts including seals, polymer gears or the roller-cage interface are representative of the isoviscous-elastic regime. The asymptotic solution [38, 39]

$$H_{\mathrm{IE}} = C_{\mathrm{IE}}(D) \cdot M^{-2/15} \tag{28}$$

can be curve fitted with

$$C_{\mathrm{IE}}(D) = -0.916 \ln\left(439\left(\frac{1}{439} + D^{-1}\right)\right) + 7.98D^{-0.192} \tag{29}$$

to represent slender elliptic contacts.

Piezoviscous-Rigid

Based on the work of Grubin [40], the following formula can be derived for the piezoviscous-rigid regime:

$$H_{\mathrm{PR}} = C_{\mathrm{PR}}(D) \cdot L^{2/3} \tag{30}$$

with

$$\begin{aligned} C_{\mathrm{PR}}(D) =& 0.441 \ln\left(-0.258\left(-\frac{1}{0.258} + D^{-1}\right)\right) + \\ & 1.11D^{-0.332}. \end{aligned} \tag{31}$$

For very slender contacts, a counter-intuitive behaviour of the film thickness can be observed: The film thickness increases with increasing load [41]. This effect takes place for piezoviscous lubricants and small to medium loads and can be observed, for example, in fig. 8. It is caused by an increased contact ellipse, which reduces side-leakage of the lubricant.
Eq. 30 cannot account for this behaviour. Therefore, a new partial solution for this regime was derived:

$$H_{\mathrm{M}} = C_{\mathrm{M}}(D) \cdot L^{2/3} M^{0.0931 - 0.00072L} \tag{32}$$

with

$$\begin{aligned} C_{\mathrm{M}}(D) = & -82.1 \ln\left(0.00618\left(\frac{1}{0.00618} + D^{-1}\right)\right) + \\ & 1.41D^{-0.528}. \end{aligned} \tag{33}$$

Eq. 32 represents contacts in between the isoviscous-rigid and the piezoviscous-rigid regime (see fig. 5). Its capability to correctly capture the physical behaviour is demonstrated by a detail analysis in fig. 4.

Piezoviscous-Elastic

Piezoviscous-elastic contacts occur, for example, in the load-zone of roller element bearings or within highly loaded gears. The asymptotic solution of this regime for point contacts of Grubin [40]

$$H_{\mathrm{PE}} = C_{\mathrm{PE}}(D) \cdot L^{3/4} M^{-1/12} \tag{34}$$

can be generalised for slender contacts with

$$C_{\mathrm{PE}}(D) = 0.205 \ln\left(439\left(\frac{1}{439} + D^{-1}\right)\right). \tag{35}$$

Discussion

The final formula for the film thickness (eq. 22) is a weighting of the contribution of different lubrication regimes. An example for the contributions of each regime towards the overall film thickness is given in fig. 5. As the load parameter M increases, it can be seen how H follows different partial solutions. Note the contributions shown in fig. 5 only represent the exemplary case of $L = 15$ and $D = 10$ and cannot be generalised.
The herein presented formula has been developed using an analogous methodology as Nijenbanning et al. [11]. Both formulas were derived for entrainment along a specific axis of the contact ellipse and do not claim to be valid for entrainment along the other axis. Nevertheless, the point contact problem ($D = 1$), as the transition between wide and slender elliptic contacts, can be calculated with both formulas.
For this reason, the predictions of both formulas are compared and plotted in fig. 6. It can be seen that the overall agreement of both formulas is very good. Yet, the formulas diverge at the transition from the isoviscous-rigid to the neighbouring regimes ($M \in [5, 20]$) and within the isoviscous-elastic regime ($L = 0$).
The new formula (eq. 22) is also tested for wide elliptic contacts ($D < 1$). Its prediction quality is poor compared to the formula of Nijenbanning et al. [11].
The asymptotic solution of the film thickness of elliptic contact for $D \to 0$ corresponds to the solution of the line contact problem. Yet, to the best of the authors' knowledge, no such solution exists in the literature for $D \to \infty$.
However, a steady decrease of the film thickness with increasing ellipticity can be observed. Physically, this can be explained by an increasing side-leakage of the fluid resulting from a shrinking minor axis of the contact ellipse [41]. This behaviour also shows in the prefactors C_i, which are monotonically decreasing functions for the ellipticity range of interest ($D \geq 1$). The theoretical case of $D = \infty$ cannot be simulated. Nonetheless, following the outlined path of reasoning, it is expected that no fluid film formation occurs and it follows

$$\lim_{D \to \infty} h(D) = 0. \tag{36}$$

This behaviour is incorporated in the new film thickness formula, since

$$\lim_{D\to\infty} C_i(D) = 0. \tag{37}$$

Additionally, a shift of the lubrication regimes towards smaller values of M with increasing D can be observed (see, for example, fig. 7 and fig. 8).
The newly derived equation is the first analytical film thickness formula for slender elliptic contacts to represent the regime of increasing film thickness with increasing load parameter M. The necessity of this detailedness, as well as the incapability of state-of-the-art formulas to capture this behaviour, can be seen very well in fig. 8.
This paper deals with the central film thickness of slender contacts, which is commonly used for friction force calculation. The minimum film thickness is also of high interest. However, the numerical parameters, simulation area and number of nodes, were increased until no further changes in the central film thickness occcured. Therefore, it cannot be guaranteed that convergence for the minimal film thickness was also achieved and the simulation results must not be used for deriving an analytical formula for the minimum film thickness. If such a formula is persued in the future, the problem of missing asymptotic solutions must be solved to obtain a formula with validity over a large parameter domain. Possible concepts for predicting the minimum film thickness in slender elliptic contacts are planned to be published in part II of this series.
The stated assumptions of the EHL simulation model improve the convergence and reduce computation time, which is essential for generation of sufficient training data. In addition, the asymptotic solutions of each regime are only valid for these assumptions. However, most lubricants do not fulfill the stated assumptions of the EHL simulation model. Therefore, the validity of the assumptions is tested for ten different contact cases and the results are listed in the appendix.
The film thickness mainly depends on the fluid condition at the inlet of the contact. Since the fluid pressure is low in this region, the impact of the chosen pressure-viscosity law is marginal as long as the reciprocal asymptotic isoviscous pressure coefficients α_p^* (eq. 4) are equivalent. This effect shows clearly when comparing simulation results obtained using either Roelands [34] or Barus pressure-viscosity laws (tab. 1). Almost all differences are within the numerical tolerance, however, a slightly higher film thickness can be observed for Roelands modelling, if small values of L occur.
The same effect can be observed for the shear-thinning behaviour. In order to verify the assumption of a Newtonian fluid, the test cases are also simulated using an Eyring fluid model

$$\eta(\dot\gamma) = \frac{\tau_\mathrm{c}}{\dot\gamma}\sinh^{-1}\left(\frac{\dot\gamma\eta_0}{\tau_\mathrm{c}}\right) \tag{38}$$

with a critical shear stress of $\tau_\mathrm{c} = 7$ MPa. Tab. 2 shows negligible differences for the central film thickness when using Newtonian and Eyring fluid models. The simulations were performed for contacts under pure rolling conditions. The effects might be more significant for contacts with high shear rates. In this case, however, thermal effects have a strong impact on the film thickness [16] and a pure study of shear-thinning becomes

irrelevant.
Attention must be paid that even though the chosen shear-thinning and pressure-viscosity models do not affect the central film thickness, these parameters influence the friction force.
By contrast, the compressibility of the lubricant has serious impact on the film thickness (tab. 3 and tab. 4). The reason for assuming incompressibility is to reduce the number of parameters within the equation. As pointed out by Vergne and Bair [25], the parameters of the Dowson and Higginson pressure-density law (eq. 14) are not universal and must be adapted to each individual lubricant. Consideration of variable pressure-density relationships would have increased the complexity unnecessarily, since a correction factor for compressibility (eq. 13) already exists. The quality of the correction factor is evaluated for different pressure-density relationships (tab. 3 and tab. 4) and good agreement with compressible EHL simulation is found, which justifies the assumption of an incompressible fluid.

Discussion on Regression Error

The training error of the newly developed film thickness formula for slender elliptic contacts (eq. 22) is 1.43 %. It is defined as the relative difference between predictions of the new formula (eq. 22) and results of EHL simulations used to obtain this equation.
Since the training error is not sufficient to estimate the quality of the new formula, it is also tested against 100 random EHL simulations. The test parameters were obtained using a latin hypercube sampling algorithm. The tested parameter range is $M \in [0.5, 10000]$, $L \in [0, 40]$ and $D \in [1, 20]$. The fluid properties, velocities and radii resulting in the dimensionless parameters M, L and D were modified for the training simulations. Due to the high computational cost of EHL simulations, only 100 were performed for testing.
The average test error is 1.34 % and the maximum test error corresponds to 4.36 %. The fact that the test and training error are almost identical is a clear indication that the number of training data points (2282) is sufficient and no overfitting occurs.
The range of tested ellipticity values ($D \in [1, 20]$) extended the training range ($D \in [1, 10]$). The average test error for simulations with $D > 10$ was 2.54 % (max. 3.98 %). This shows that the quality of the newly derived formula declines when being extrapolated to even more slender contacts. However, it can still predict the film thickness solidly. Extrapolation of M and L was not tested, since convergence would have been critical, especially for more extreme values of M.
The preferable quality for slender elliptic contacts of the new film thickness formula in comparison to the approaches of Chittenden et al. [12] and Nijenbanning et al. [11] can also be seen in fig. 7 and fig. 8. It must be emphasised that the shown EHL simulation results were not part of the training set of this study.
Experimental validation of the new analytical formula with interferometry measurements exists and is planned to be published in part II of this series.

Conclusion

State-of-the-art analytical central film thickness equations were benchmarked for elliptic contacts with entrainment along the major axis of the contact ellipse (slender contacts) against multi-level EHL simulations. The results show an unambiguous necessity for an improved analytical formula with validity over a great parameter domain.
Therefore, a new analytical central film thickness formula for slender elliptic contacts was developed. Asymptotic solutions for each lubrication regime are the basis of the film thickness equation. The main advantages of the new formula are

- large number of training data (2282 simulations)
- wide range of ellipticity ratios ($D \in [1, 10]$) has been adopted
- no limitation on L and M parameter domain by incorporation of asymptotic solutions
- agreement with EHL simulations (avg. test error of 1.34 %)
- improved prediction quality compared to literature film thickness equations [11, 28]
- first formula to incorporate the effect of rising film thickness with increasing load

The model is based on the listed assumptions. Assumptions concerning the fluid behaviour were tested and only minor influence was found for the pressure-viscosity relationship and the shear-thinning behaviour. Compressibility has a significant impact on the film thickness, but currently available correction factors (eq. 13) can properly represent these effects.

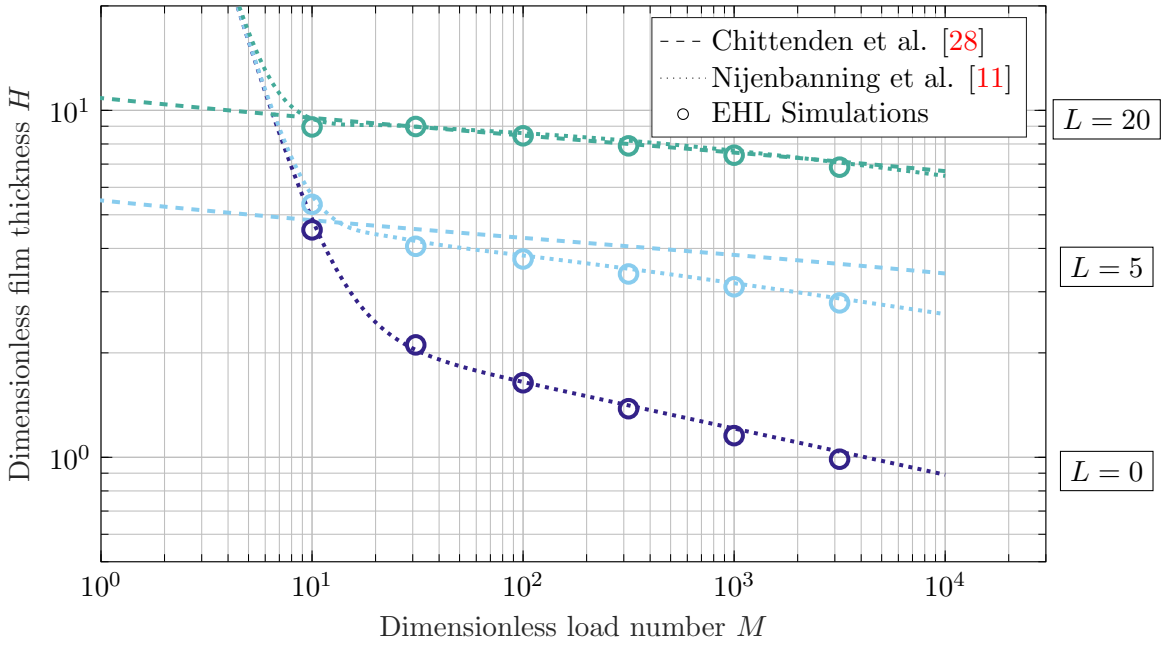

Figure 1: Benchmarking of state-of-the-art film thickness formulas for wide elliptic contacts ($D = 0.25$).

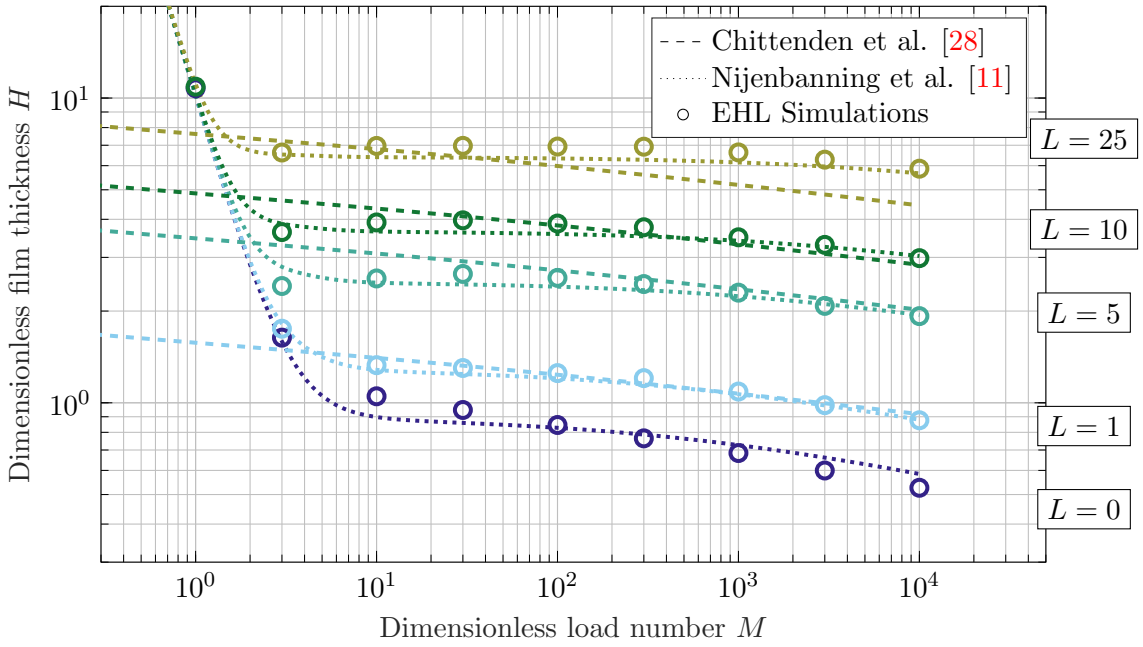

Figure 2: Benchmarking of state-of-the-art film thickness formulas for an ellipticity ratio of $D = 2$.

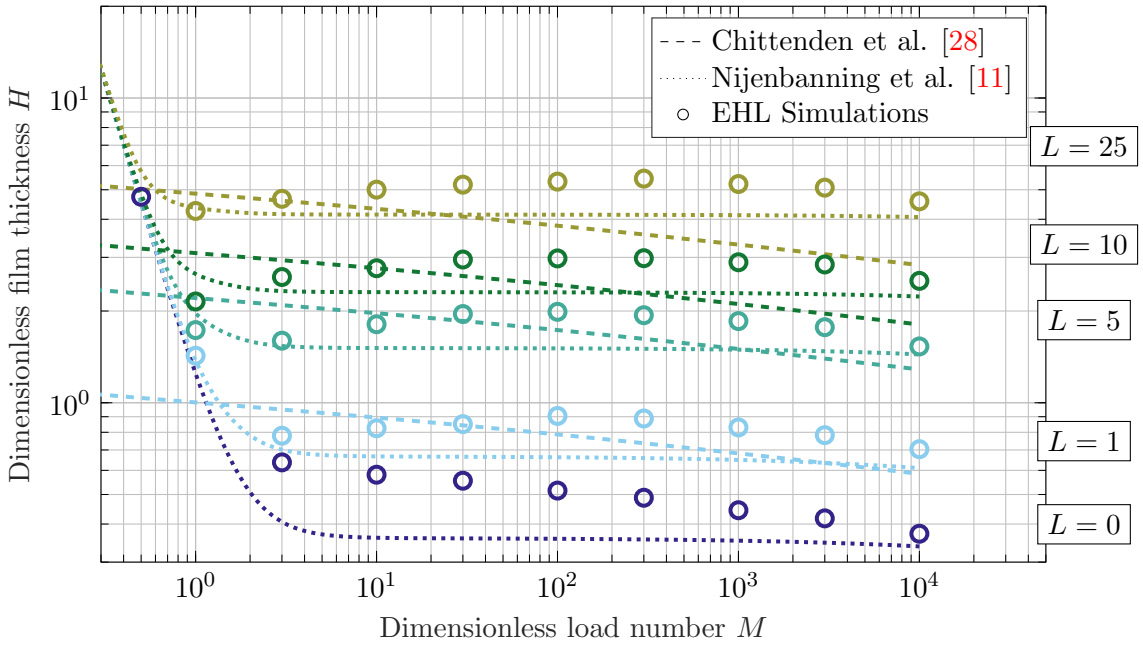

Figure 3: Benchmarking of state-of-the-art film thickness formulas for an ellipticity ratio of $D = 5$.

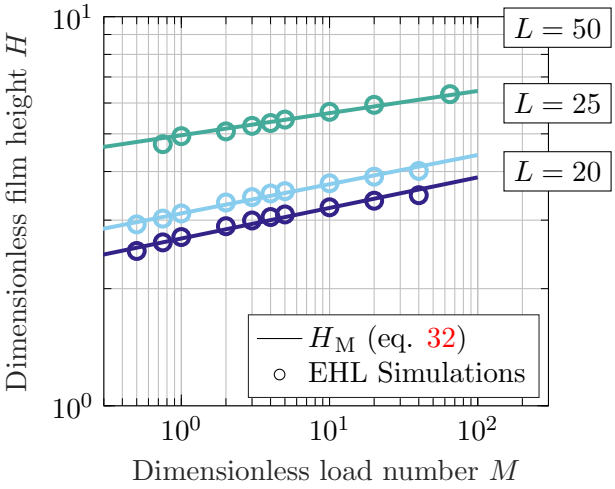

Figure 4: Validation of partial solution H_{M} (eq. 32) for regime of increasing H with increasing M for $D = 10$.

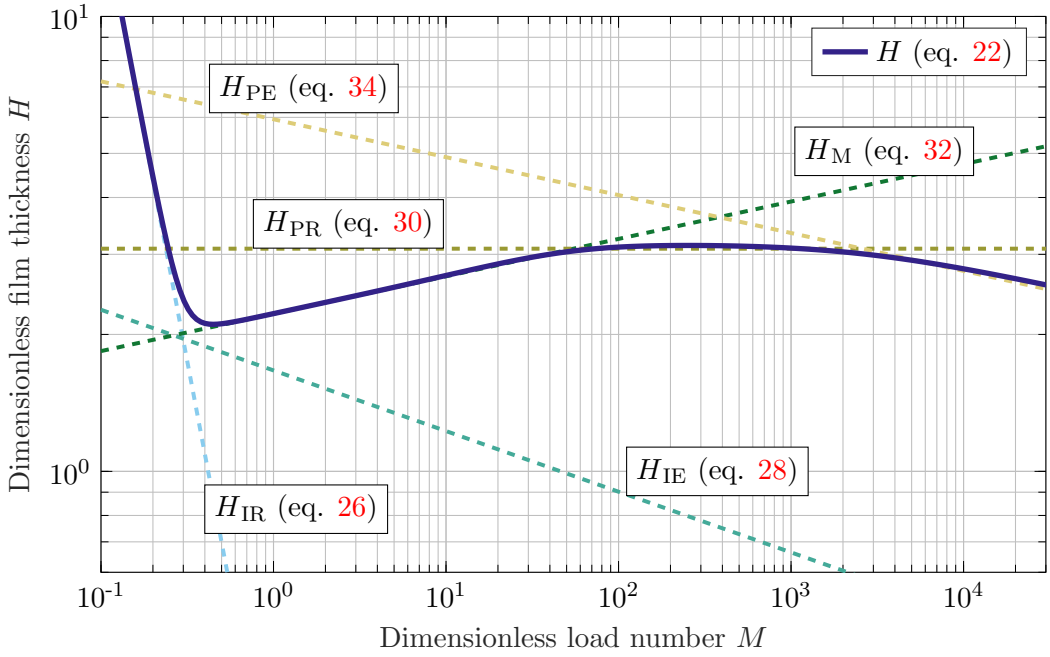

Figure 5: Contributions of the different lubrication regimes to the overall film thickness according to eq. 22, for $L = 15$ and $D = 10$.

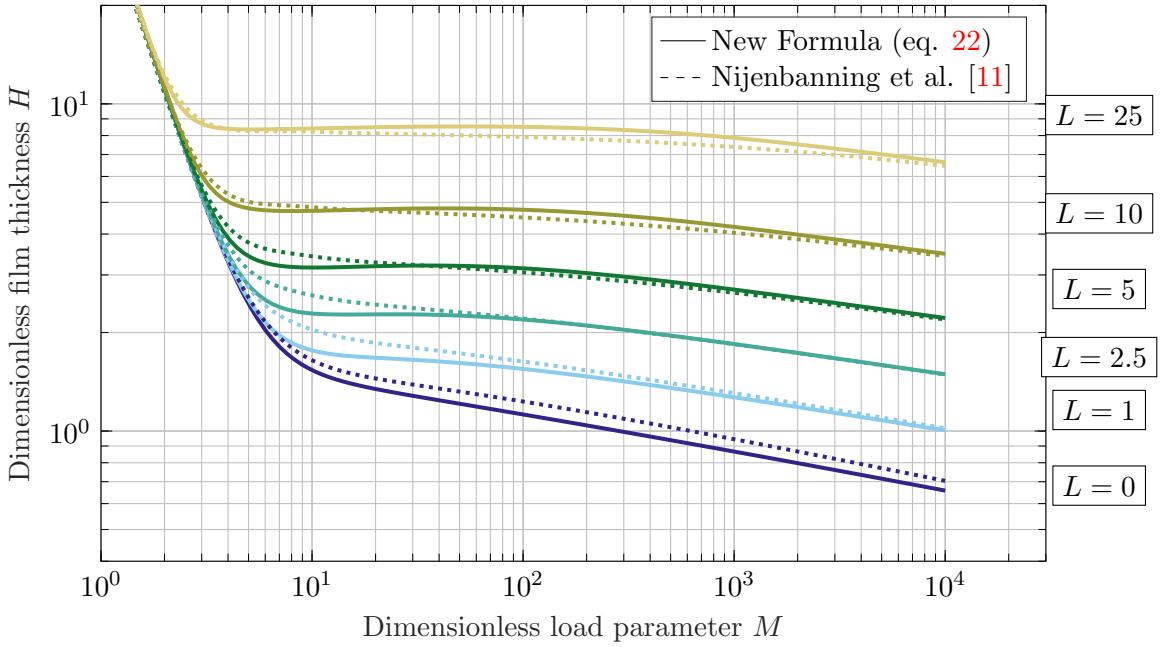

Figure 6: Comparison of the new film thickness formula (eq. 22) against the formula of Nijenbanning et al. [11] for point contacts ($D = 1$).

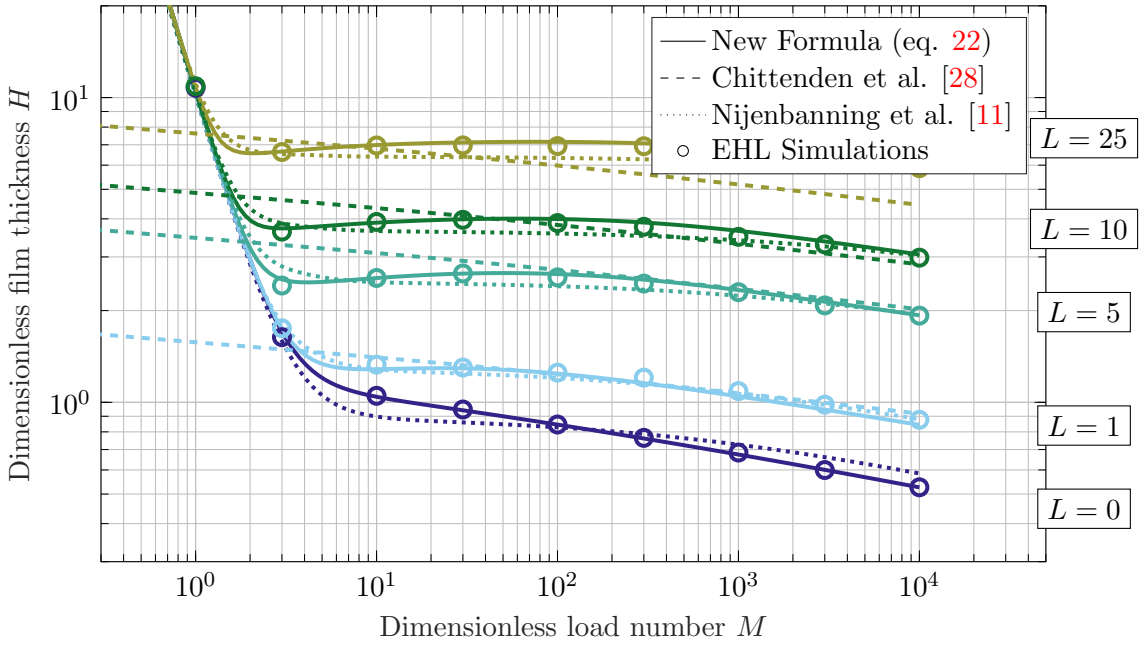

Figure 7: Comparison of the new film thickness equation (eq. 22) against the film thickness formulas of Chittenden et al. [12] and Nijenbanning et al.[11] for an ellipticity ratio of $D = 2$.

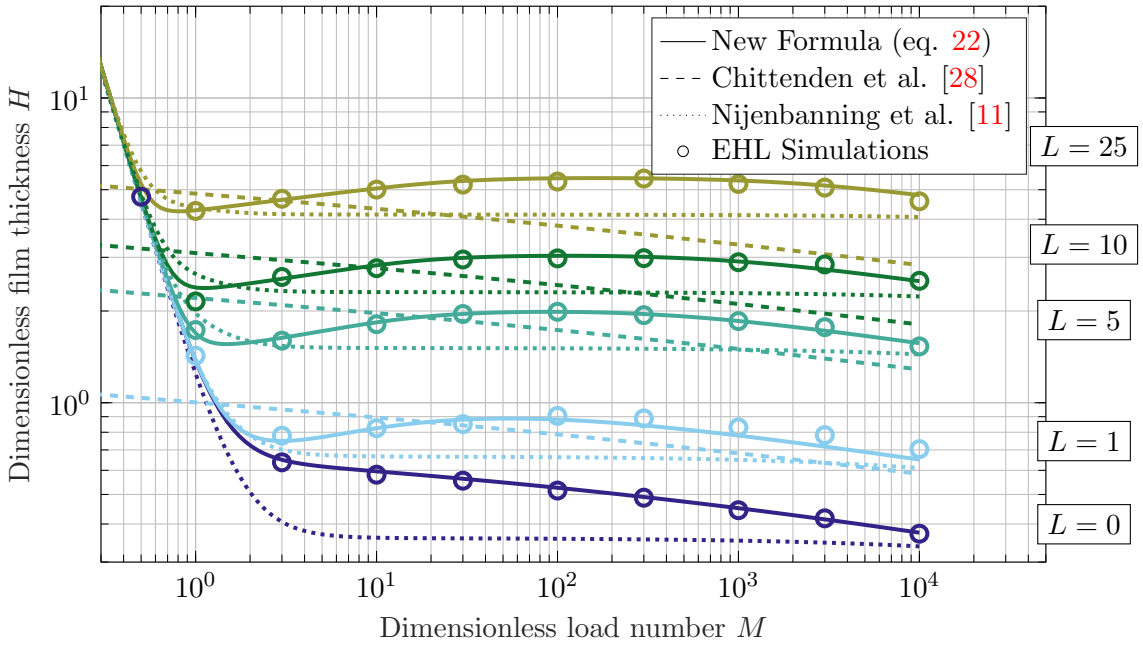

Figure 8: Comparison of the new film thickness equation (eq. 22) against the film thickness formulas of Chittenden et al. [12] and Nijenbanning et al.[11] for an ellipticity ratio of $D = 5$.

Bibliography

[1] Dowson D, Higginson GR. New Roller Bearing Lubrication Formula. Engineering. 1961;192:158–159.

[2] Dowson D, Toyoda S. A Central Film Thickness Formula for Elastohydrodynamic Line Contacts. Proceedings of the Fifth Leeds-Lyon Symposium on Tribology. 1978;p. 60–64.

[3] Hamrock BJ, Dowson D. Isothermal Elastohydrodynamic Lubrication of Point Contacts: Part I—Theoretical Formulation. Journal of Lubrication Technology. 1976;98(2):223–228.

[4] Hamrock BJ, Dowson D. Isothermal Elastohydrodynamic Lubrication of Point Contacts: Part II—Ellipticity Parameter Results. Journal of Lubrication Technology. 1976;98(3):375–381.

[5] Hamrock BJ, Dowson D. Isothermal elastohydrodynamic lubrication of point contacts: part III—fully flooded results. Journal of Lubrication Technology. 1977;99(2):264–275.

[6] Hamrock BJ, Dowson D. Isothermal elastohydrodynamic lubrication of point contacts: Part IV — starvation results. Journal of Lubrication Technology. 1977;99(1):15–23. Available from: https://doi.org/10.1115/1.3452973.

[7] Lubrecht AA, Venner CH, Colin F. Film thickness calculation in elastohydrodynamic lubricated line and elliptical contacts: The Dowson, Higginson, Hamrock contribution. Proc Inst Mech Eng, Part J. 2009;223(3):511–515. Available from: https://doi.org/10.1243/13506501JET508.

[8] Ranger AP, Ettles CMM, Cameron A. The Solution of the Point Contact Elasto-Hydrodynamic Problem. Proceedings of the Royal Society of London Series A, Mathematical and Physical Sciences. 1975;346(1645):227–244. Available from: http://www.jstor.org/stable/78929.

[9] Zhu D, Wang Q. Elastohydrodynamic Lubrication: A Gateway to Interfacial Mechanics - Review and Prospect. Journal of Tribology. 2011 10;133.

[10] Moes H. Optimum similarity analysis with applications to elastohydrodynamic lubrication. Wear. 1992;159(1):57 – 66. Available from: http://www.sciencedirect.com/science/article/pii/004316489290286H.

[11] Nijenbanning G, Venner CH, Moes H. Film thickness in elastohydrodynamically lubricated elliptic contacts. Wear. 1994;176(2):217 – 229. Available from: http://www.sciencedirect.com/science/article/pii/0043164894901503.

[12] Chittenden RJ, Dowson D, Dunn JF, Taylor CM, Johnson KL. A theoretical analysis of the isothermal elastohydrodynamic lubrication of concentrated contacts. I. Direction of lubricant entrainment coincident with the major axis of the Hertzian contact ellipse. Proceedings of the Royal Society of London A Mathematical and Physical Sciences. 1985;397(1813):245–269. Available from: https://royalsocietypublishing.org/doi/abs/10.1098/rspa.1985.0014.

[13] Wheeler JD, Vergne P, Fillot N, Philippon D. On the relevance of analytical film thickness EHD equations for isothermal point contacts: Qualitative or quantitative predictions? Friction. 2016;4(4):369–379.

[14] Moes H. Lubrication and Beyond. Enschede: University of Twente; 2000.

[15] Venner CH, Lubrecht AA. Revisiting film thickness in slender elastohydrodynamically lubricated contacts. Proc Inst Mech Eng, Part C. 2010;224(12):2549–2558. Available from: https://doi.org/10.1243/09544062JMES2316.

[16] Kaneta M, Kawashima R, Masuda S, Nishikawa H, Yang P, Wang J. Thermal effects on the film thickness in elliptic EHL contacts with entrainment along the major contact axis. Journal of Tribology. 2002 Apr;124(2):420–427. Available from: https://doi.org/10.1115/1.1430675.

[17] Wolf M, Sanner A, Fatemi A. A semi-analytical approach for rapid detection of roller-flange contacts in roller element bearings. Proc Inst Mech Eng, Part J. 2020;Available from: https://doi.org/10.1177/1350650120964295.

[18] Shirzadegan M, Björling M, Almqvist A, Larsson R. Low degree of freedom approach for predicting friction in elastohydrodynamically lubricated contacts. Tribology International. 2016;94:560–570. Available from: https://www.sciencedirect.com/science/article/pii/S0301679X15004594.

[19] Shirzadegan M, Larsson R, Almqvist A. A low degree of freedom approach for prediction of friction in finite EHL line contacts. Tribology International. 2017;115:628–639. Available from: https://www.sciencedirect.com/science/article/pii/S0301679X17303079.

[20] Otero JE, de la Guerra Ochoa E, Tanarro EC, del Rio Lopez B. Friction coefficient in mixed lubrication: A simplified analytical approach for highly loaded non-conformal contacts. Advances in Mechanical Engineering. 2017;9(7):1687814017706266. Available from: https://doi.org/10.1177/1687814017706266.

[21] Masjedi M, Khonsari MM. An engineering approach for rapid evaluation of traction coefficient and wear in mixed EHL. Tribology International. 2015;92:184–190. Available from: https://www.sciencedirect.com/science/article/pii/S0301679X15002121.

[22] Venner CH, Napel W. Multilevel solution of the elastohydrodynamically lubricated circular contact problem Part I: Theory and numerical algorithm. Wear. 1992;152(2):351 – 367. Available from: http://www.sciencedirect.com/science/article/pii/004316489290132R.

[23] Venner CH, Lubrecht AA. Multi-level methods in lubrication. 1st ed. Dowson D, editor. Elsevier; 2000.

[24] Wang W. EHL, Full Numerical Solution Methods. In: Wang QJ, Chung YW, editors. Encyclopedia of Tribology. Boston, MA: Springer US; 2013. p. 852–859. Available from: https://doi.org/10.1007/978-0-387-92897-5_630.

[25] Vergne P, Bair S. Classical EHL Versus Quantitative EHL: A Perspective Part I-Real Viscosity-Pressure Dependence and the Viscosity-Pressure Coefficient for Predicting Film Thickness. Tribol Lett. 2014 04;54(1):1–12.

[26] Blok H. Inverse Problems in Hydrodynamic Lubrication and Design Directives for Lubricated Flexible Surfaces. Proc Int'l Symp Lub and Wear, Houston. 1963;7. Available from: https://ci.nii.ac.jp/naid/10026701153/en/.

[27] Venner CH, Napel W. Multilevel solution of the elastohydrodynamically lubricated circular contact problem part II: Smooth surface results. Wear. 1992;152(2):369 – 381. Available from: http://www.sciencedirect.com/science/article/pii/004316489290133S.

[28] Chittenden RJ, Dowson D, Dunn JF, Taylor CM, Johnson KL. A theoretical analysis of the isothermal elastohydrodynamic lubrication of concentrated contacts. II. General case, with lubricant entrainment along either principal axis of the Hertzian contact ellipse or at some intermediate angle. Proceedings of the Royal Society of London A Mathematical and Physical Sciences. 1985;397(1813):271–294. Available from: https://royalsocietypublishing.org/doi/abs/10.1098/rspa.1985.0015.

[29] Evans HP, Snidle RW. The Isothermal Elastohydrodynamic Lubrication of Spheres. Journal of Lubrication Technology. 1981 10;103(4):547–557. Available from: https://doi.org/10.1115/1.3251734.

[30] Masjedi M, Khonsari MM. On the effect of surface roughness in point-contact EHL: Formulas for film thickness and asperity load. Tribology International. 2015 Feb;82:228–244. Available from: http://www.sciencedirect.com/science/article/pii/S0301679X1400334X.

[31] Canzi A, Venner CH, Lubrecht AA. Film thickness prediction in elastohydrodynamically lubricated elliptical contacts. Proc Inst Mech Eng, Part J. 2010;224(9):917–923. Available from: https://doi.org/10.1243/13506501JET717.

[32] Marian M, Bartz M, Wartzack S, Rosenkranz A. Non-Dimensional Groups, Film Thickness Equations and Correction Factors for Elastohydrodynamic Lubrication: A Review. Lubricants. 2020;8(10). Available from: https://www.mdpi.com/2075-4442/8/10/95.

[33] van Leeuwen H. The determination of the pressure–viscosity coefficient of a lubricant through an accurate film thickness formula and accurate film thickness measurements. Proc Inst Mech Eng, Part J. 2009 12;223(8):1143–1163.

[34] Hamrock BJ, Schmid SR, Jacobson BO. Fundamentals of Fluid Film Lubrication. 2nd ed. Faulkner LL, editor. New York: Marcel Dekker, Inc.; 2004.

[35] Lugt PM, Morales-Espejel GE. A Review of Elasto-Hydrodynamic Lubrication Theory. Tribology Transactions. 2011;54(3):470–496. Available from: https://doi.org/10.1080/10402004.2010.551804.

[36] Dowson D, Higginson GR. Elastohydrodynamic lubrication, the fundamentals of roller and gear lubrication. Oxford: Pergamon Press; 1966.

[37] Johnson KL. Regimes of Elastohydrodynamic Lubrication. Journal of Mechanical Engineering Science. 1970;12(1):9–16. Available from: https://doi.org/10.1243/JMES_JOUR_1970_012_004_02.

[38] Hamrock BJ, Dowson D. Elastohydrodynamic lubrication of elliptical contacts for materials of low elastic modulus I—fully flooded conjunction. J of Lubrication Tech. 1978 Apr;100(2):236–245. Available from: https://doi.org/10.1115/1.3453152.

[39] Crook AW. The lubrication of rollers II. Film thickness with relation to viscosity and speed. Philosophical Transactions of the Royal Society of London Series A, Mathematical and Physical Sciences. 1961;254(1040):223–236.

[40] Grubin A. Fundamentals of the hydrodynamic theory of lubrication of heavily loaded cylindrical surfaces. Investigation of the Contact Machine Componets. 1949;2.

[41] Wheeler JD, Fillot N, Vergne P, Philippon D, Morales-Espejel GE. On the crucial role of ellipticity on elastohydrodynamic film thickness and friction. Proc Inst Mech Eng, Part J. 2016 Mar;230(12):1503–1515. Available from: https://doi.org/10.1177/1350650116637583.

Nomenclature

b, c	parameters of Dowson and Higginson pressure-density law
C	Prefactor of asymptotic solution
D	ellipticity ratio
E'	reduced young's modulus, $1/E' = 0.5((1-\nu_1^2)/E_1 + (1-\nu_2^2)/E_2)$
E_i	young's modulus of body i
F_{N}	normal force
G	dimensionless material parameter (Moes)
$\tilde{H}$	dimensionless film thickness
H	dimensionless film thickness (Moes)
h	film thickness
H_{00}	curvefit parameter
L	dimensionless material parameter
M	dimensionless load parameter (Moes)
p	pressure
R_i	reduced radius of curvature in i direction, $1/R_i = 1/R_{i,1} + 1/R_{i,2}$
s, t	curvefit parameters for isoviscous-piezoviscous transition
U	dimensionless speed parameter
u_0	sum velocity, $u_0 = u_1 + u_2$
u_i	velocity of body i
W	dimensionless load parameter
α	Barus parameter

α_{p}^{*} reciprocal asymptotic isoviscous pressure coefficient

η viscosity

$\dot{\gamma}$ shear rate

ν_i poisson's ratio of body i

ρ mass density

θ angle between entrainment velocity and major axis of contact ellipse

Indices

x Direction along major axis of contact ellipse

y Direction along minor axis of contact ellipse

0 atmospheric pressure

1,2 body 1, body 2

C Chittenden

com compressible

e entrainment direction

H Hertzian

IE isoviscous-elastic

inc incompressible

IR isoviscous-rigid

M regime of increasing film thickness with increasing load parameter

N Nijenbanning

PE piezoviscous-elastic

PR piezoviscous-rigid

s direction transverse to entrainment

Appendix

Table 1: Dimensionless central film thicknesses obtained by EHL simulations using Barus (H_{Barus}) and Roelands (H_{Roel}) pressure-viscosity laws.

No.	M	L	D	α_{p}^{*} in GPa^{-1}	H_{Barus}	H_{Roel}	Rel. Difference in %
1	95.4	15.2	3.2	28.3	4.493	4.495	0.03
2	9.7	27.5	1.7	51.23	7.772	7.763	0.12
3	39.9	20.1	4.2	37.4	4.863	4.86	0.07
4	1936	22.2	4.0	41.4	5.123	5.118	0.1
5	76.5	8.04	1.7	15.0	3.627	3.6	0.74
6	1663	6.54	2.2	12.2	2.598	2.646	1.81
7	7345	34.9	1.9	62	7.567	7.553	0.18
8	1689	14.5	8.1	27.1	3.236	3.237	0.04
9	3013	21.9	7.9	40.8	4.204	4.2	0.09
10	77.8	3.15	2.1	5.88	2.069	2.148	3.71

Table 2: Dimensionless central film thicknesses obtained by EHL simulations using Newtonian (H_{Newton}) and Eyring (H_{Eyring}) shear-thinning laws.

No.	M	L	D	H_{Newton}	H_{Eyring}	Rel. Difference in %
1	95.4	15.2	3.2	4.493	4.493	0.02
2	9.7	27.5	1.7	7.772	7.76	0.15
3	39.9	20.1	4.2	4.863	4.865	0.03
4	1936	22.2	4.0	5.123	5.115	0.16
5	76.5	8.04	1.7	3.627	3.619	0.22
6	1663	6.54	2.2	2.598	2.604	0.23
7	7345	34.9	1.9	7.567	no convergence	no convergence
8	1689	14.5	8.1	3.236	3.226	0.31
9	3013	21.9	7.9	4.204	4.235	0.73
10	77.8	3.15	2.1	2.069	2.058	0.52

Table 3: Dimensionless central film thicknesses obtained using EHL simulations assuming incompressible (H_{inc}) or compressible ($H_{\mathrm{comp,EHL}}$) fluids. Compressible fluids are modelled via eq. 14 with $b = 5.9 \times 10^8$ Pa and $c = 1.34$. Results are compared to incompressible film thicknesses corrected via eq. 13 ($H_{\mathrm{comp,corr}}$).

No.	M	L	D	H_{inc}	$H_{\mathrm{comp,EHL}}$	$H_{\mathrm{comp,corr}}$ (eq. 13)	Rel. Difference in %
1	95.4	15.2	3.2	4.49	3.71	3.63	2.0
2	9.7	27.5	1.7	7.77	6.54	6.73	2.85
3	39.9	20.1	4.2	4.86	4.04	3.97	1.59
4	1936	22.2	4.0	5.12	3.96	3.95	0.26
5	76.5	8.04	1.7	3.63	3.06	2.99	2.29
6	1663	6.54	2.2	2.6	2.11	2.02	4.35
7	7345	34.9	1.9	7.57	6.16	5.81	5.75
8	1689	14.5	8.1	3.24	2.52	2.48	1.83
9	3013	21.9	7.9	4.2	3.22	3.21	0.51
10	77.8	3.15	2.1	2.07	1.78	1.7	4.66

Table 4: Dimensionless central film thicknesses obtained using EHL simulations assuming incompressible (H_{inc}) or compressible ($H_{\mathrm{comp,EHL}}$) fluids. Compressible fluids are modelled via eq. 14 with $b = 4 \times 10^8\,\mathrm{Pa}$ and $c = 1.15$. Results are compared to incompressible film thicknesses corrected via eq. 13 ($H_{\mathrm{comp,corr}}$)

No.	M	L	D	H_{inc}	$H_{\mathrm{comp,EHL}}$	$H_{\mathrm{comp,corr}}$ (eq. 13)	Rel. Difference in %
1	95.4	15.2	3.2	4.49	4.08	4.03	1.34
2	9.7	27.5	1.7	7.77	7.0	7.18	2.52
3	39.9	20.1	4.2	4.86	4.45	4.38	1.65
4	1936	22.2	4.0	5.12	4.52	4.51	0.26
5	76.5	8.04	1.7	3.63	3.36	3.28	2.36
6	1663	6.54	2.2	2.6	2.38	2.29	3.47
7	7345	34.9	1.9	7.57	6.67	6.65	0.38
8	1689	14.5	8.1	3.24	2.87	2.84	1.18
9	3013	21.9	7.9	4.2	3.7	3.68	0.39
10	77.8	3.15	2.1	2.07	1.95	1.87	4.31